อิทธิพลของปริมาณการเชื่อมโยงต่อการตกผลึกเมื่อยืดและความแข็งแรงของยางธรรมชาติที่วัลคาไนซ์ด้วยกำมะถัน

INFLUENCE OF CROSSLINK DENSITY ON STRAIN-INDUCED CRYSTALLIZATION AND STRENGTH OF SULPHUR-VULCANIZED NATURAL RUBBER

วัชรินทร์ สายน้ำใส[1*], กฤษฎา สุชีวะ[2], ชิยูกิ โตกิ[3]
WATCHARIN SAINUMSAI[1*], KRISDA SUCHIVA[2], SHIGEYUKI TOKI[3]

บทคัดย่อ

งานวิจัยนี้ได้ศึกษาผลของปริมาณการเชื่อมโยงต่อการตกผลึกเมื่อยืดและความแข็งแรงของยางธรรมชาติที่วัลคาไนซ์ด้วยกำมะถัน พบว่าที่ปริมาณการเชื่อมโยงต่ำๆ แทบจะไม่มีผลต่อระยะยืดที่เริ่มเกิดการตกผลึก แต่ที่ปริมาณการเชื่อมโยงสูงขึ้น (สูงกว่า $8x10^{-5}$ mole/cm^3) ระยะยืดที่เริ่มเกิดการตกผลึกจะลดลงเล็กน้อยเมื่อปริมาณการเชื่อมโยงสูงขึ้น ดัชนีการตกผลึกจะสูงขึ้นเมื่อปริมาณการเชื่อมโยงสูงขึ้นจนถึงจุดหนึ่งหลังจากนั้นค่าจะต่ำลง ความแข็งแรงของยางขึ้นอยู่กับปริมาณการเชื่อมโยงเช่นกัน ดัชนีการตกผลึกจะสูงขึ้นตามระยะยืดจนกระทั่งคงที่ที่ประมาณ 1.5 ในขณะที่ความเค้นดึงยังคงสูงขึ้นเรื่อยๆ แม้ว่าปริมาณการตกผลึกจะมีค่าคงที่แล้วก็ตาม นั่นแสดงว่าความแข็งแรงของยางไม่ได้ขึ้นโดยตรงกับการตกผลึกเมื่อยืด แต่เป็นผลมาจากการจัดเรียงตัวอย่างเป็นระเบียบของโซ่โมเลกุล โดยเฉพาะส่วนที่เชื่อมต่อกับโครงสร้างผลึก

คำสำคัญ: ยางธรรมชาติ, การตกผลึกเมื่อยืด, สมบัติเชิงกล, การกระเจิงของรังสีเอ็กซ์เรย์

Abstract

The present work is concerned with the study of the effect of crosslink density of sulphur-vulcanized natural rubber (NR) on strain-induced crystallization (SIC) and tensile strength of NR. It was found that the crosslink density has almost no effect on the onset of SIC for low crosslink density, but for high crosslink density (above $8x10^{-5}$ mole/cm^3), the onset of SIC showed slight decrease. The strain-induced crystallinity index was found to increase with increasing crosslink density then decreased. Tensile strength showed similar dependence on the crosslink density. The crystallinity index developed reaches a constant value of about 1.5 even at high strain. Since the stress still continues to rise even after the degree of crystallinity reaches a constant value, it was proposed that the high tensile strength of NR vulcanizate is not the direct consequence of SIC as is widely believed but is due to orientation of the molecular segments, particularly those connected to the crystalline structures.

Keywords: natural rubber, strain-induced crystallization, mechanical properties, WAXD.

[1]Lecturer, Rubber and Polymer Technology Program, Faculty of Science and Technology, Songkhla Rajabhat University, Songkhla, 90000, Thailand

[2]Assistant Professor, Rubber Technology Research Centre, Faculty of Science, Mahidol University, Nakorn Pathom, 73170 Thailand.

[3]Researcher, Department of Chemistry, State University of New York at Stony Brook, NY, 11794-3400, USA

[*]**Corresponding author, E-mail:** sainumsai2512@hotmail.com

Introduction

Natural rubber (NR) vulcanizates show great physical and mechanical properties in tensile strength and fatigue resistance, together with high hysteresis energy [1]. Since these characteristics take place without addition of any filler. In particular, its high tensile strength (20-30 MPa) and large strain at break (8.0-10.0) are excellent in comparison with the case of unfilled SBR (Styrene Butadiene Rubber) vulcanizate where the tensile strength is about 1.5-2.0 MPa and the strain at break is 4.0-5.0. These superior properties of NR have been assumed to be due to its strain-induced crystallization (SIC) ability [2-5]. Therefore, the study on SIC behavior of crosslinked NR is the most importance for elucidating the mechanical characteristics of NR.

The strain-induced crystallization in NR has been observed and studied by X-ray diffraction since 1925 [6]. The increase of strain-induced crystallization in NR with strain had been studied extensively [7-11]. The simultaneous measurements of the stress-strain relation and the strain-induced crystallization by wide angle X-ray diffraction (WAXD) using a conventional X-ray instrument [12] revealed that the hysteresis of stress-strain relation is caused by the strain-induced crystallization. The results show that the strain-induced crystallization decreases the stress since the length of amorphous molecule along the stretching direction increases due to its crystallization.

Synchrotron X-ray and modified stretching machine make it clear to show the both hysteresis in the stress-strain relation and in the strain-induced crystallization in rubbers and to elucidate the stress decrease by the onset of strain-induced crystallization [13-21]. The experimental results agree with classical thermo-mechanical theories on strain-induced crystallization [22-23] that suggested the onset of strain-induced crystallization decrease the stress before the upturn of stress.

Sulphur vulcanizated rubbers have network structures that are mainly composed of monosulphidic, disulphidic, and polysulphidic crosslinks. The structures including the crosslink densities and types of vulcanizates are very important parameters because of their dominant effects on the mechanical properties. The ratio of polysulphidic, disulphidic and monosulphidic crosslinks depends on the ratio of sulphur to the accelerators, cure time and the kind of accelerator in the formulation. The crosslink has been considered to be vital for SIC since the theory of rubber elasticity of polymer crosslink network has applied to elucidate SIC at thermo-mechanical equilibrium state. In this paper, we focus on the role of crosslink. Five levels of crosslink density are studied.

Experimental

Materials.

Commercial grade of Standard Thai Natural Rubber Light (STR-5L) was compound with many formulae shown in Table 1. All the ingredients including sulphur and accelerator were mixed on a laboratory-scale 6-in. roll mill. Vulcanization was carried out in an electrically heated hydraulic press at 150°C using the optimum cure time (T_{c90}) previously determined with a moving die rheometer (TechPro MD+) at 150°C following ASTM D-5289.

Table 1 Composition and sample preparation conditions of the samples.

Ingredients	Quantity [phr]				
	CV1	CV2	CV3	CV4	CV5
STR-5L	100	100	100	100	100
Zinc Oxide	5	5	5	5	5
Stearic acid	1	1	1	1	1
CBS[a]	0.19	0.56	0.75	0.94	1.31
Sulphur	0.50	1.50	2.00	2.50	3.50
Cure time[b] [min]	31	16	13	12	11

[a]CBS (N-cyclohexyl-2-benzothiazole sulphenamide), [b]Curing temperature 150°C

Determination of crosslink:

Equilibrium swelling in toluene was used to determine the crosslink densities of the rubber vulcanizates. The Crosslink density was determined using the method described by Cunneen and Russell [24]. The molecular weight of the network chain between chemical crosslinks for a phantom network, M_c; is expressed by the Flory–Rehner relationship [25-26]:

$$M_c = \frac{-2\rho_r V_s (V_r^{1/3} - V_r/2)}{[\ln(1-V_r) + V_r + \chi V_r^2]} \quad (1)$$

where V_r is the volume fraction of rubber in the swollen sample, V_s is the molar volume of the swelling solvent, ρ_r is the density of the rubber sample, and χ is the rubber-solvent interaction parameter. The values of the constant used in the above calculation were V_s = 10^7 cm^3/mole and χ = 0.393 [27]. The total crosslink density (ν_T) is given by [28]

$$\nu_T = \frac{1}{2M_c} \quad (2)$$

Measurements of stress-strain curves and tensile strength:

Tensile properties of NR vulcanizates were measured according to ASTM D-412 using a universal testing machine (Instron 5569 series, Norwood, USA) at 25°C. The rate of deformation was 500 mm/min.

Strain-induced crystallization measurement:

In-situ wide-angle X-ray diffraction (WAXD) measurements were carried out at the X27C beamline in the National Synchrotron Light Source (NSLS), Brookhaven National Laboratory (BNL). The wavelength of X-ray was 0.1371 nm. An MAR-CCD X-ray detector (made by MAR, USA) was used to record the two-dimensional wide-angle X-ray diffraction (WAXD) patterns for quantitative image analyses. The typical image acquisition time for each scan was 30 sec. The data analysis software package (POLAR) used was developed by Stony brook Technology and Applied Research at Stony Brook, New York. The tensile machines allowed the symmetric stretching of the sample, permitting the focused X-ray to illuminate the same sample position during deformation. The chosen deformation rate was 10 mm/min. The stress-strain curves during extension were collected at 25°C in the uniaxial deformation mode.

Results and Discussion

Stress–strain curves of NR vulcanizates with various crosslink densities are shown in Fig. 1. The sample with the larger crosslink density showed the higher modulus in the tensile measurements of this study (Table 2). In the lower strain region, the modulus is low and slowly increases with the increase in strain; when the strain is larger, the upturn in stress. The sample with the larger crosslink density showed the upturn in stress at lower strain.

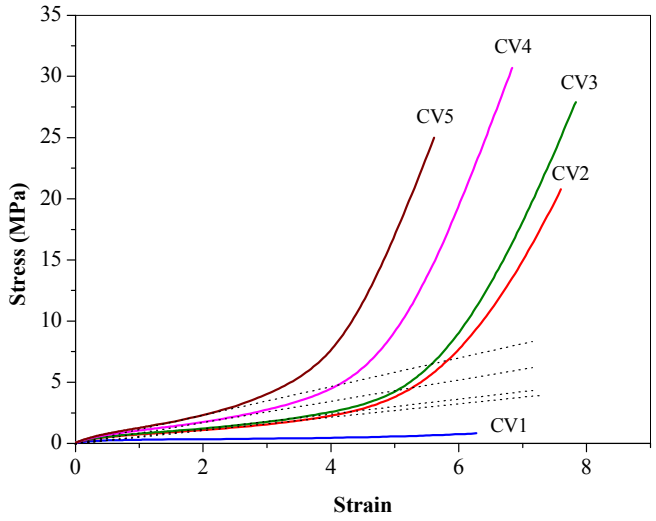

Fig. 1 Tensile stress-strain curves of NR vulcanizates with various crosslink densities.

Table 2 Total crosslink densities and mechanical properties of the samples.

Sample	CV1	CV2	CV3	CV4	CV5
ν_T [a] [x 10^{-5} mol/cm^3]	0.5	5.6	7.8	8.7	11.3
M1 [b] [MPa]	0.3	0.7	0.8	1.0	1.3
M3 [c] [MPa]	0.4	1.5	1.9	2.7	4.1
TS [d] [MPa]	0.9	20.5	28.7	30.6	24.9
Strain at break	6.2	7.6	7.5	6.9	5.8

[a]Total crosslink density, [b]Modulus at strain 1.0, [c]Modulus at strain 3.0, [d]Tensile strength

The stress-strain curve and selected 3D WAXD patterns during deformation (at a 10 mm/min rate) of sample CV3 at 25°C are shown in Fig. 2. Each WAXD image is taken at the strain indicated by the arrow. The high intensity of synchrotron X-rays made it possible to collect the WAXD patterns during deformation in real time without holding the sample still. It was seen that stress generally increased with strain. In Fig. 2, it is seen that 3D WAXD patterns exhibited an amorphous halo below strain 3.0, while its intensity distribution shifted slightly toward the equator with increasing strain (e.g., strain 3.0). At strain 4.0, the deformation of the halo pattern became more intense, and several weak but distinct crystalline reflections are seen. These reflections are sharp and highly oriented and appeared in smaller numbers than those in fully

crystallized patterns (e.g., at strains 5 and more). These reflections are caused by the first-formed strain-induced crystallites, which are defective in crystalline ordering or registration but highly oriented with respect to the stretching direction. This finding is consistent with the fringemicelle crystal model induced by strain during deformation of rubber recently proposed by Toki and coworkers [5,15-16,18-19]. In contrast, at strains above 4 (e.g., strains 5.0 and more), the WAXD patterns exhibited well oriented crystalline reflections from a monoclinic unit cell with parameters similar to a = 1.25 nm, b = 0.89 nm, c = 0.81 nm, and γ = 92°, as previously reported by Bunn [8]. It is interesting to see that, even at strains 5.0 and more, one can observe the persistence of the unoriented amorphous halo, which is consistent with the finding that a substantial amount of amorphous chains remain unstretched at high extension [5,15,18].

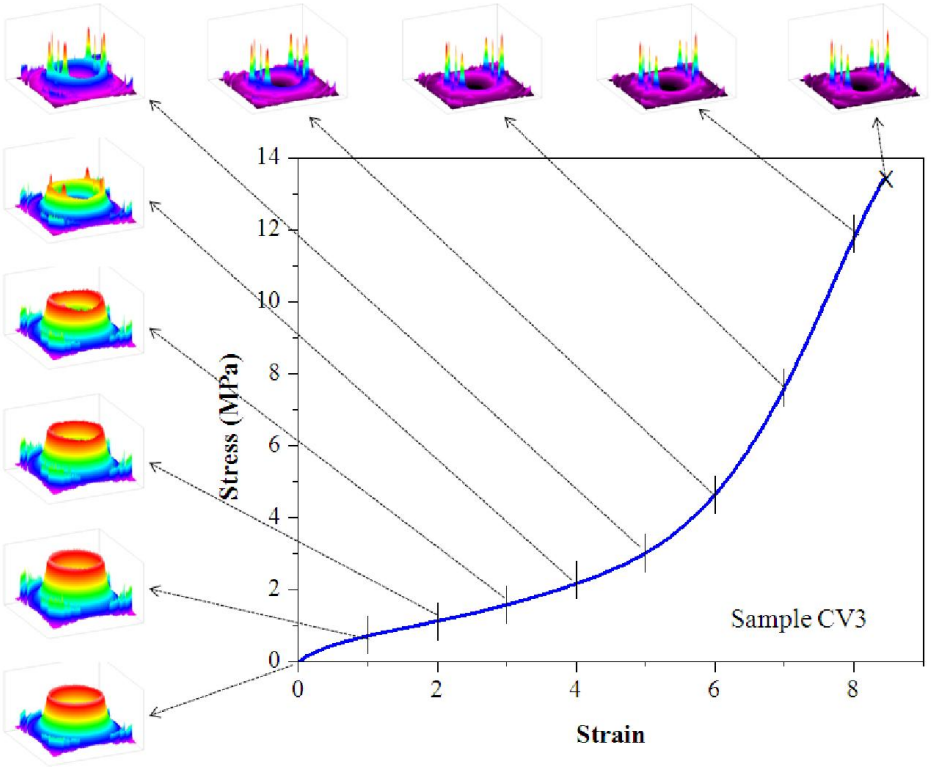

Fig. 2 The stress-strain relationship and selected WAXD patterns in 3D expression of the sample CV3. Each image was taken at the average strain indicated by the arrows.

WAXD patterns can be analyzed into three fractions such as crystal, oriented amorphous and unoriented amorphous. (The procedure to analyze the data is mentioned elsewhere [5,15-21]). The integral intensities as a function of scattering vector “s” at each strain are shown in Fig. 3. It is clear that the anisotropic fraction increases with strain smoothly.

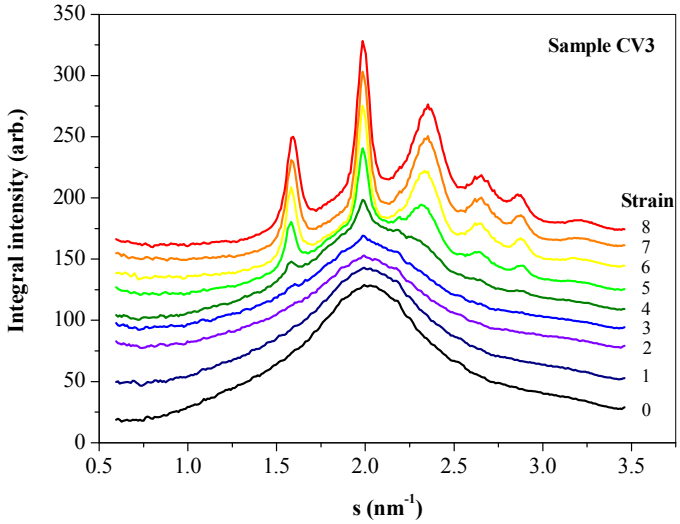

Fig. 3 1D cylindrical intensity profiles as a function of scattering vector “s” of the sample CV3.

From the integrated intensity patterns, we can evaluate crystallinity index and oriented amorphous index as shown in Fig. 4. Crystallinity index increases with strain during deformation. The oriented amorphous index does not increase significantly and seems to be a precursor of strain-induced crystallization. The tendencies are similarly observed in pure vulcanized NR and pure vulcanized IR [5,15-21]. From the above observation, we can conclude that the oriented amorphous chains are precursors to the induced crystals. The crystallization rate from the oriented chains must be very fast, probably in the order of 60 m/s, as reported by Mitchell and Meier [29]. In addition, it is reasonable to rationalize that the strain-induced crystallites are in the extended chain crystal form having a microfibrillar structure. As only a small fraction of chains are oriented and crystallized, this suggests that the strain-induced crystallites form an additional physical crosslinking network, carrying most of the applied load. The above results indicate that even under a very high deformation state, the majority of the chains remain unoriented. This behavior seems to be very universal in rubbery materials.

The variations of the crystallinity index of NR vulcanizates with various crosslink densities during deformation at 25°C are shown in Fig. 5. It is found that the crystallinity index starts to increase at strain around 2.5 in all samples. The crosslink density had only negligible influence on the onset strain of crystallization (Table 3). At strain = 3.0, the crystallinity index is almost identical. At strain larger than 3, the crystallinity index becomes dominant. NR vulcanizates with various crosslink densities showed similar trends. The crystallization started after the sample is elongated to some extent. The sample with the larger crosslink density typically exhibited a steeper slope in the plot. It is interesting to find that the rate of SIC is the faster for the samples with the higher crosslink density.

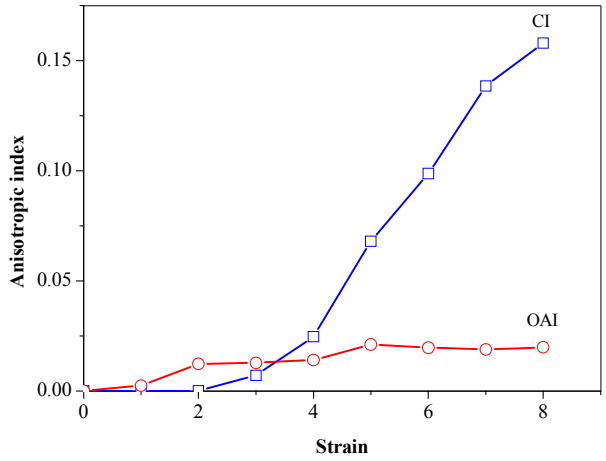

Fig. 4 The anisotropic fractions (oriented amorphous and crystal) of the sample CV3 at each strain during deformation.

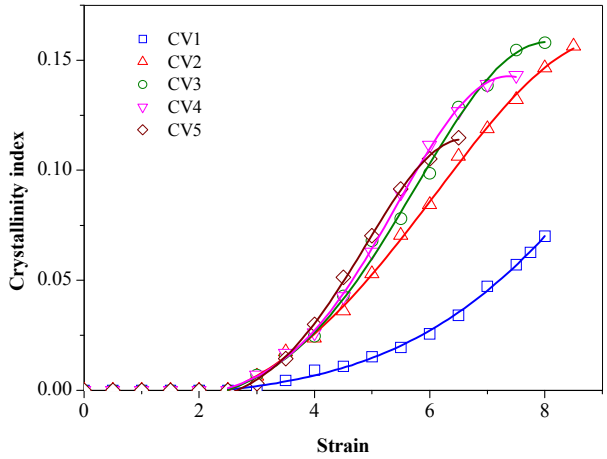

Fig. 5 Relationship between crystallinity index and tensile strain of NR vulcanizates with various crosslink densities.

Table 3 Crystallization rate, incipient strain of crystallization and strain at upturn stress of the samples.

Sample	Crystallization rate [min^{-1}]	Onset strain of crystallization	Strain at upturn stress
CV1	0.014	2.45	-
CV2	0.029	2.55	3.9
CV3	0.035	2.55	3.6
CV4	0.036	2.63	2.9
CV5	0.036	2.37	2.3

The crystallization rate reflects a relative SIC rate and was obtained from the slope of linearly increasing part of the curve in Fig. 5 (slope in the strain dependence of anisotropic fraction). In contrast to the almost no effect of crosslink density on the onset of SIC, the crosslink density was found to have definite influence on the rate of SIC as shown in Table 3. The rate of SIC showed linearly increases with increasing crosslink density up to the value of $8x10^5$ mole/cm^3. Further increasing of the crosslink density resulted in a nearly constant of the rate of crystallization.

The upturn of stress in the stress-strain curve of NR vulcanizate has popularly been attributed to SIC [30]. Results of the present study suggest otherwise. It can be seen that the crystallinity index developed approximately reaches a constant value at about 1.5 even at the large strain at which stress-upturn is observed. The results of the present study, thus, indicate that stress-upturn and the high tensile strength of NR vulcanizate are not the direct consequence of SIC. For rubbery materials, this stress-upturn is generally associated with the stress at which the smallest chains reach their critical extensibility [31]. Therefore, it appears that molecular orientation along the applied stress is responsible for the observed upturn of stress at a certain strain and also the final strength of the vulcanized rubber. SIC may contribute to the high strength by facilitating the formation of orientation of either molecules or crystals, increasing the rubber's ability to bear force. Thus, further studies on SIC and orientation of sulphur-vulcanized NR samples are necessary in order to understand better the factors that are responsible for high strength of strain-crystallizable rubbers.

Conclusion

In the NR samples vulcanizates with CV curing system an increase in the total crosslink densities, tensile strength and crystallinity index are increased up to maximum, then decreased. The NR vulcanizates with the larger crosslink density showed the upturn in stress at lower strain. The crosslink density had only negligible influence on the onset strain of crystallization. The rate of SIC is the faster for the samples with the higher crosslink density.

Acknowledgments

I would like to thank all professors and staff of NSLS, BNL at State University of New York (Stony Brook) for their help and support when running fast time-resolved synchrotron wide angle x-ray diffraction (WAXD) experiments.

References

[1] Gent, A. N. (1992). Engineering with rubber, Oxford University Press, Oxford, U.K..

[2] Mark, J. E., Erman, B., & Eirich, F.R. (Eds.), (1994). Science and Technology of rubber, second ed., Academic Press, San Diego.

[3] Roberts, A. D. (1988). Natural Rubber Science and Technology, Oxford University Press, Oxford, U.K.

[4] Murakami, S., Senoo, K., Toki, S., & Kohjiya S. (2002). Polymer. 43, 2117–2120.

[5] Toki, S., Sics, I., Ran, S., Liu, L., Hsiao, B. S., Murakami, S., Senoo, K., & Kohjiya, S. (2002). Macromolecules. 35, 6578–6584.

[6] Katz, J. R. (1925). Die Naturwissenschaften. 13, 410-416.

[7] Gehman, S. D., & Field, J. E. (1939) J.Appl. Phys. 10, 564-572.

[8] Bunn, C. W. (1941). Proc. Roy. Soc. A 180, 40-66.
[9] Luch, D., & Yeh, G. S. Y. J. (1973). Macromolecular Sci. B 7, 121-155.
[10] Shimomura, Y., & White, J. L. (1982). J. Appl. Polym. Sci. 27, 3553.
[11] Mitchell, G. R. (1984). Polymer 25, 1562-1572.
[12] Toki, S., Fujimaki, T., & Okuyama, M. (2000). Polymer 41, 5423-5429.
[13] Murakami, S., Senoo, K., Toki, S., & Kohjiya, S. (2002). Polymer 43, 2117-2120.
[14] Toki, S., Sics, I., Ran, S., Liu, L., Hsiao, B. S., Murakami, S., Senoo, K., & Kohjiya, S. (2002). Macromolecules 35, 6578-6584.
[15] Toki, S., Sics, I., Ran, S., Liu, L., & Hsiao, B. S. (2003). Polymer 44, 6003-6011.
[16] Toki, S. & Hsiao, B. S. (2003). Macromolecules 36, 5915-5917.
[17] Tosaka, M., Murakami, S., Poompradub, S., Kohjiya, S., Ikeda, Y., Toki, S., Sics, I., & Hsiao, B. S. (2004). Macromolecules 37, 3299-3309.
[18] Toki, S., Sics, I., Hsiao, B. S., Murakami, S., Tosaka, M., Poompradub, S., Kohjiya, S., & Ikeda, Y. (2004). J. Polym. Sci., Part B: Polym. Phys. 42, 956-964.
[19] Toki, S., Sics, I., Hsiao, B. S., Murakami, S., Tosaka, M., Poompradub, S., Kohjiya, S., & Ikeda, Y. (2004). Rubber Chem. Technol. 77, 317-335.
[20] Toki, S., Sics, I., Hsiao, B. S., Murakami, S., Tosaka, M., Poompradub, S., Kohjiya, S., & Ikeda, Y. (2005). Macromolecules 38, 7064-7073.
[21] Tosaka, M., Kohjiya, S., Murakami, S., Poompradub, S., Ikeda, Y., Toki, S., Sics, I., & Hsiao, B. S. (2004). Rubber Chem. Technol. 77, 711-723.
[22] Flory, P. J. J. (1947). Chem. Phys. 15, 397-408.
[23] Bekkedahl, N., & Wood, L. A. (1941). Ind. Eng. Chem. 33, 381-384.
[24] Cunneen, J. I., & Russell, R. M. (1970). Rubber Chem. Technol. 43, 1215.
[25] Flory, P. J. J., & Rehner, J. J. (1943). Chem. Phys. 11, 521-526.
[26] Flory, P. J. J. (1950). Chem. Phys. 18, 108-111.
[27] Brydson, J. A. (1978). Rubber Chemistry, Applied Science Publishers Ltd., London.
[28] Blow C. M. (Ed.), (1975). Rubber Technology and Manufacture, Newness Butterworths, London.
[29] Mitchell, J. C., & Meier, D. J. (1968). J. Polym. Sci. A-2 6, 1689-1703.
[30] Versloot, P., van Duin, M., Duynstee, E. F. J., Haasnoot, J. G., Put, J., & Reedijk, J. (1992). Rubber Chem. Technol. 64, 343.
[31] Chenal, J. M., Chazeau, L., Guy, L., Bomal, Y., & Gauthier, C. (2007). Polymer 48, 1042-1046.